Erratum: Pressure melting of ice [J. Chem. Phys. 80, 438 (1984)]

Thomas A. Weber and Frank H. Stillinger
AT&T Bell Laboratories, Murray Hill, New Jersey 07974

The pages of our article were printed out of sequence. To read the article in a coherent manner the pages should be read in the following order: pp. 438, 440, 441, 439, 442, and 443.

Erratum: J. Chem. Phys. 81, 3363 (1984)

 0021-9606/84/193363-01$02.10

Pressure melting of ice

Thomas A. Weber and Frank H. Stillinger
Bell Laboratories, Murray Hill, New Jersey 07974

(Reviewed 31 May 1983; accepted 23 September 1983)

A 250-molecule ice Ih crystallite has been melted at a pressure of about 2 kbars using molecular dynamics computer simulation. The ST2 potential has been used to represent molecular interactions. Melting was observed to begin at the crystallite surface and to proceed inward until the entire crystal was converted to an amorphous droplet. The melting point was found to be depressed by about 23 °C at 2 kbars in comparison with a corresponding calculation at ambient pressure. Quenches from various thermodynamic states were created to study the inherent structures in the fluid. Approximately 80%–90% of the latent heat of melting is due to the difference in the packing structures of the fluid compared to the crystal; the remainder may be ascribed to the greater anharmonicity of the fluid over the crystal.

I. INTRODUCTION

Water has been studied extensively by computer simulation using both the molecular dynamics and Monte Carlo methods, and consequently valuable insight has been gained about the nature of the liquid[1–7] and solid[8,9] phases. In the various studies, many different potentials have been used to model the molecular interactions. These range from simple rigid-molecule interactions such as the ST2 potential[2] to more complex potentials which allow for molecular vibrations and chemical reactivity.[10] Considering the obvious importance of phase transitions, it is indeed surprising that only recently has the phase behavior of water been examined via molecular dynamics simulation.[11] A necessary but not sufficient test of any potential used to model water is that the density should increase as melting occurs. A corollary to this, of course, is that applying pressure to the crystal should cause its melting point to decrease. In this paper, we extend our previous studies on ice crystal melting at low pressure to report here the melting of an ice crystal under substantial applied pressure. In addition, we continue in our effort to understand the nature and role of amorphous structures in governing the mechanically stable packings of water molecules by performing nonannealing quenches from various thermodynamic states generated in the melting studies.

The computer simulations (detailed in Sec. II) are performed on small clusters of 250 ST2 water molecules constrained by an external potential. These studies differ from the procedure normally followed in molecular dynamics simulations in that no periodic boundary conditions are applied and also in that no cutoffs on the force are used. It is essential that the clusters have a free surface because ice melting is normally initiated at the surface and proceeds inward to the center of the crystal. In our previous simulation of ice melting[11] we had applied a weak external potential which prevented the droplet from evaporating as melting occurred and which acted as a nonwetting container for the cluster. We now use this same potential function with suitably modified parameters to compress the droplet. Although the requirement of no cutoffs on the force makes the calculations more difficult, this is necessary to maintain the validity of the calculations, particularly since the droplet has a free surface.

In Sec. III, we discuss the thermodynamic properties of the cluster as a function of temperature. We find as in our previous simulations that the crystal starts to melt at the surface and that the melting proceeds inward to the core region until the entire ice crystal structure is consumed. We also find that the pressure produces a depression of the melting point.

In Sec. IV, we detail the results of some very rapid quenches of various thermodynamic states produced in following the crystal-melting and fluid-heating curve. About 80%–90% of the latent heat of melting is attributable to the upward shift in the potential energy as the underlying inherent structures shift from regular packings to amorphous packings.

This paper ends with a discussion of the results and the remaining important issues.

II. DYNAMICS

The transition between the hexagonal ice I and the liquid state has been previously studied using the ST2 potential to describe the pair interaction between water molecules.[11] An additional external wall potential has been used to keep the cluster bounded in size and location, and to keep the droplet compressed. The ST2 potential was chosen to model the water because it has the following advantages: (i.) it is a simple potential form whose properties have been well characterized by extensive simulations; (ii.) it treats the water molecule as a rigid asymmetric rotor; (iii.) it realistically accounts for hydrogen bonding; (iv.) it successfully reproduces the thermodynamic anomalies of bulk liquid water.[2,11]
The wall potential was chosen to have the following form:

$$U(r_i) = \cosh(ar_i)/\cosh(ar_0), \tag{2.1}$$

where r_i is the distance of the center of mass of the ith molecule from the origin. The parameter a was chosen to be 2 Å^{-1} and U as written is given in kcal/mol. For the high pressure melting r_0 was chosen to be 12 Å (our previous study used the value 20 Å). This choice for r_0 produces a

 0021-9606/84/010438-06$02.10

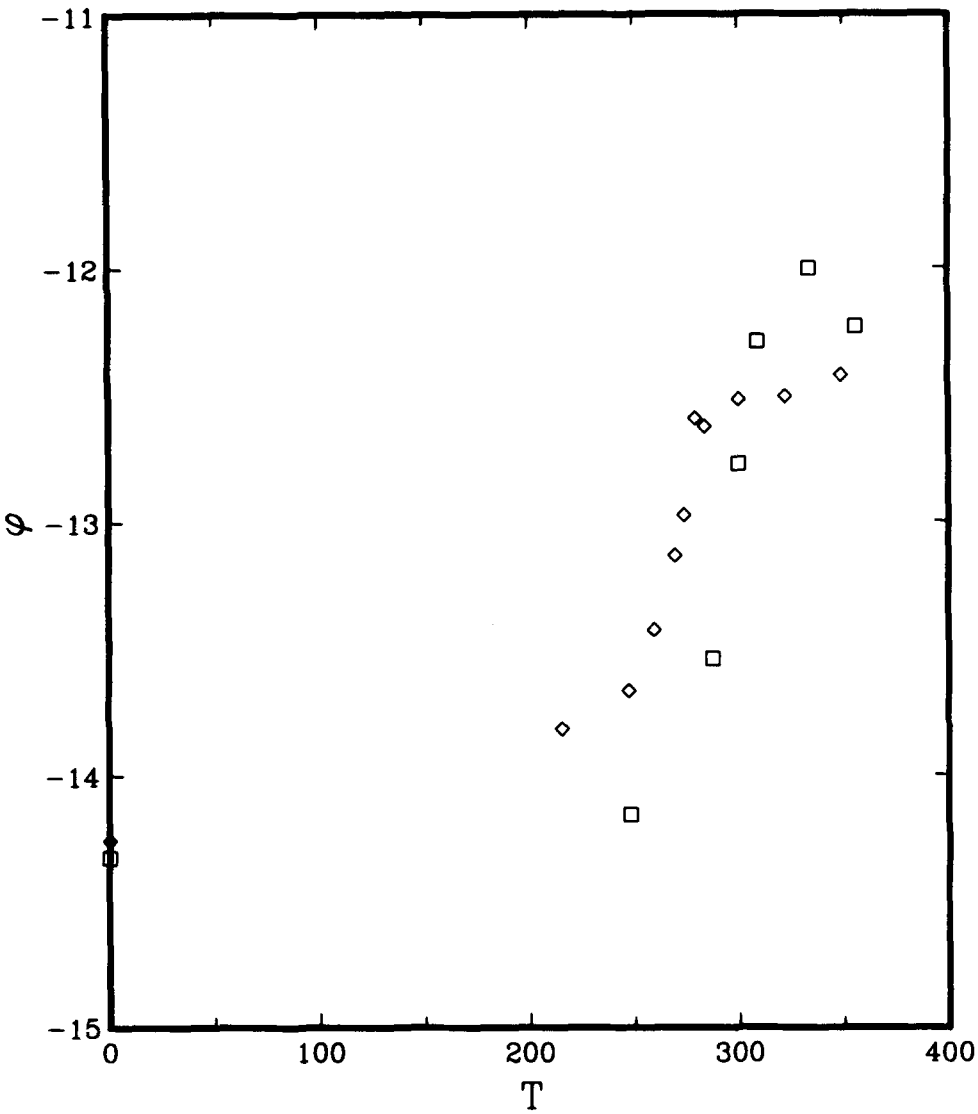

FIG. 2. The potential energy per particle of those molecules in the core region ϕ_c as a function of temperature. The squares show the melting curve at 0 kbars while the diamonds show melting at ~2 kbars.

In our low pressure simulations of ice melting we have probed a few structures and have shown their importance in accounting for the latent heat of melting and possibly in explaining the low temperature supercooling anomalies of water.

The construction of the discrete minima of the system is carried out in a simple and straightforward fashion. For any given system configuration $\mathbf{x} = \mathbf{x}_1, \mathbf{x}_2, \mathbf{x}_3, \ldots \mathbf{x}_N$, there is a mapping M which takes the system to its relative minimum in Φ, and we denote this configuration by α,

$$M(\mathbf{x}) = \alpha. \tag{4.1}$$

This mapping may be generated from solutions to

$$\frac{d\mathbf{x}}{dt} = -\nabla\Phi(\mathbf{x}) \tag{4.2}$$

since this function begins at $\mathbf{x}$ and converges to α along a path of steepest descent. Note that M is not defined at the saddle points of the configurational space, but these points constitute a set of zero measure and may be disregarded for our purpose.

The thermodynamic states generated in the molecular dynamics simulations provide a convenient means of probing a few of the inherent structures (i.e., Φ minima) available to the fluid. The final configuration of each state reported in Table I was numerically quenched (without permitting annealing) to its local potential energy minimum. Although in principle Eq. (4.2) may be solved directly to determine the minima, another approach was utilized to improve computational efficiency. We first apply a strong damping term to the equations of motion of the system for a period of 0.5 ps. This removes most of the kinetic energy and allows the molecules to settle quickly into a rough approximation of the inherent structure without annealing. Next, a conjugate gradient procedure[18] is applied so as to determine quickly the precise configuration of the local minimum. Even so the calculations are very time consuming: About 7 h of CRAY-1 time are required to completely quench one state.

Table II lists the potential energy per particle for the quench configurations. In addition the number of hydrogen bonds, as defined earlier by the energy criterion, is given for each configuration at the Φ minimum. A plot of the quench energy per particle vs initial "fictive" temperature is shown in Fig. 1. The potential energy per particle of the quenched

more nearly spherical cluster than previously, as measured by the droplet moments of inertia, and it subjects the unmelted cluster to a pressure of about 2.7 kbars at 0 K.

The initial configuration for the low pressure melting study was produced by excising a spherical droplet composed of 250 water molecules from a perfect infinite crystal of ice I. The infinite crystal was produced by periodically replicating a unit cell composed of eight water molecules. The hydrogen-bonded molecular arrangement within the unit cell was constructed such that the net dipole vanished. After the droplet was produced the molecular dynamics (with vanishing initial momenta) was started so that surface water molecules were allowed to reorient and relax. The system was then slowly brought down to 0 K by momentum scaling. To produce the high-pressure-droplet starting configuration the r_0 parameter was slowly decreased from 20 to 12 Å while simultaneously removing the kinetic energy produced by the compression. The system was then quenched to 0 K to produce the initial crystal configuration.

The pressure is estimated from the wall virial B_v using the equation

$$P = \frac{2}{3} B_v / V, \tag{2.2}$$

where V is the droplet volume and the wall virial for the potential of Eq. (2.1) is

$$B_v = \frac{1}{2} a \sum_{j=1}^{N} \frac{\langle r_j \sinh(a r_j) \rangle}{\cosh(a r_0)}. \tag{2.3}$$

The volume for the crystal is assumed to scale as the cube of the average nearest-neighbor oxygen–oxygen distance $\bar{r}_{oo}$. At a density of 0.9419 g/cm^3, $\bar{r}_{oo}$ is 2.752 63 Å.[16] Using these estimates, the pressure in kbars is found from

$$P = 1.395\,407 \times 10^{-6} \left[\frac{2.752\,63}{\bar{r}_{oo}} \right]^3 B_v, \tag{2.4}$$

where $\bar{r}_{oo}$ is in Å and B_v is in kcal/mol. The average $\bar{r}_{oo}$ distance is extracted as the average of the 12 shortest oxygen–oxygen distances for the particles nearest the center of the cluster.

The equations of motion for the ST2 potential were solved numerically using the Evans method of quaternion variables.[12] This method eliminates the singularities present in the straightforward solution of the coupled Euler–Lagrange equations of motion. The time step was taken to be 4×10^{-4} ps, which was adequate to maintain reasonably accurate conservation of energy. As already mentioned above, all pairwise interactions between ST2 water molecules were explicitly handled and no cutoffs were applied.

Starting with the 0 K configuration, the system was heated by scaling the rotational and translational momenta. The system was equilibrated at each temperature by running the trajectory for 0.5 ps. Then dynamical averages were collected by running at a given energy for either 2 or 4 ps. In the transition region where the melting process was underway, we ran for 4 ps to insure that the system was fully relaxed. In this way the droplet was heated stepwise to 350 K. The final configuration for each state was then quenched by a procedure which will be discussed subsequently.

TABLE I. Cluster properties.[a]

E	t	P	T	$\langle \mu^2 \rangle^{1/2}$	$\langle I \rangle$
− 12.137 826	0.0	2.76	0.00	15.60	4.551
− 9.181 365	2.0	2.25 ± 0.13	215.45	17.63	4.505
− 8.687 656	2.0	2.05 ± 0.17	247.64	18.71	4.491
− 8.439 618	2.0	1.91 ± 0.14	259.70	13.81	4.453
− 8.188 822	4.0	1.80 ± 0.11	269.74	12.81	4.422
− 7.938 645	4.0	1.53 ± 0.11	273.90	15.44	4.344
− 7.688 356	4.0	1.34 ± 0.17	279.42	20.34	4.266
− 7.438 227	4.0	1.15 ± 0.14	284.00	17.20	4.127
− 7.187 998	2.0	1.07 ± 0.08	300.18	18.07	4.107
− 6.688 012	2.0	1.08 ± 0.07	322.27	15.94	4.103
− 6.187 709	2.0	1.31 ± 0.14	349.48	20.37	4.164

[a] E [kcal/mol], t [ps], P [kbar], T [K], μ[D], $\langle I \rangle$ [10^{-35} g cm^2].

III. CLUSTER MELTING

Table I lists the properties of the eleven states generated in the melting of the hexagonal ice. The table lists the average total energy of the state, the length of simulation time over which averages were calculated, the pressure and mean temperature (calculated from the translational and rotational kinetic energy) and the average moment of the inertia. Unlike the simulations of the low pressure clusters where the ratio of the largest to the smallest moment typically was 1.4, the three inertial moments for the high pressure simulations are nearly equal. This change stems from the inhibition of droplet surface waves by the stringently confining external potential that is now present.

Table II lists the average number of hydrogen bonds $\langle n_H \rangle$ for each state. As before[11] we have employed an energy criterion to define hydrogen bonding. Any two molecules whose ST2 interaction potential falls below − 4 kcal/mol are considered to be hydrogen bonded. The average potential energy per particle

$$\langle \phi \rangle = E - 3kT \tag{3.1}$$

is also listed in the table. A plot of the average potential energy per particle is shown in Fig. 1.

For the purpose of analysis, the cluster has been divided into two regions, a core and a mantle. The core consists of all water molecules, N_c in number, whose center of mass lies

TABLE II. Quenches for 250-molecule cluster under pressure.[a]

			Quench state	
T	$\langle n_H \rangle$	$\langle \phi \rangle$	n_H	ϕ_q
0.00	439	− 12.137 826	439	− 12.137 826
215.45	331	− 10.466 186	426	− 12.060 135
247.64	323	− 10.164 440	422	− 12.033 032
259.70	301	− 9.988 321	414	− 11.967 342
269.74	285	− 9.797 409	402	− 11.856 292
273.90	265	− 9.572 028	401	− 11.701 041
279.42	248	− 9.354 658	394	− 11.696 689
284.00	232	− 9.131 841	384	− 11.636 793
300.18	215	− 8.978 100	393	− 11.546 466
322.27	198	− 8.609 847	386	− 11.605 959
349.48	177	− 8.271 809	362	− 11.425 676

[a] T [K], ϕ [kcal/mol].

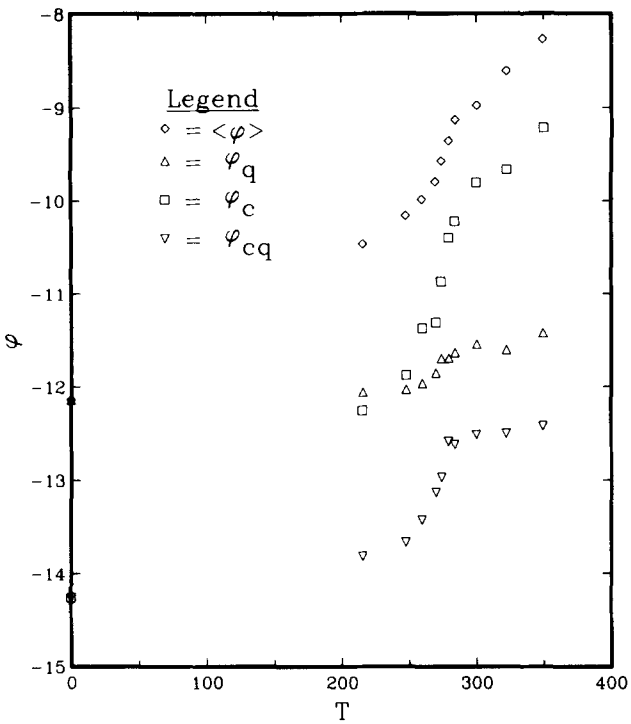

FIG. 1. Potential energy per particle as a function of temperature. $\langle\phi\rangle$ is the potential energy per particle averaged over the entire length of the simulation. ϕ_q is the potential energy per particle of the quenched configuration. ϕ_c is the potential energy per particle of those molecules in the core region (see the text for definition of core region). ϕ_{cq} is the potential energy per particle of those molecules in the core region of the quenched configuration.

within 9 Å of the origin. All other molecules by default are considered to be in the mantle region.

The potential energy per particle of the core molecules is

$$\phi_c = \frac{1}{2N_c}\sum_{i=1}^{N_c}\sum_{j=1}^{N} V^{(2)}(i,j), \tag{3.2}$$

where $V^{(2)}(i,j)$ is the total interaction potential between molecules i and j. It is assumed that the molecules are labeled such that the first N_c reside in the core and the remainder reside in the mantle. Half of the interaction energy between a molecule in the core and one in the mantle is assigned to the core.

TABLE III. Properties of the cluster-core subset.[a]

	Initial configuration		Quenched configuration	
T	N_c	ϕ_c	N_c	ϕ_{cq}
0.00	94	− 14.256 437	94	− 14.256 437
215.45	95	− 12.255 947	100	− 13.818 827
247.64	100	− 11.879 409	101	− 13.669 612
259.70	100	− 11.373 032	102	− 13.429 062
269.74	97	− 11.312 879	106	− 13.134 692
273.90	103	− 10.875 553	115	− 12.974 653
279.42	112	− 10.402 666	113	− 12.592 829
284.00	112	− 10.224 682	118	− 12.625 084
300.18	113	− 9.805 785 5	112	− 12.519 750
322.27	112	− 9.662 913 9	119	− 12.506 452
349.48	115	− 9.211 560 2	118	− 12.423 240

[a] ϕ_c [kcal/mol].

ϕ_c (from the end of each run) vs T is listed in Table III and plotted in Fig. 1. The plot of ϕ_c shows a sharper break at the melting point than $\langle\phi\rangle$ indicating that the core remains substantially crystalline until the melting point whereas the mantle premelts well below the bulk crystal melting point. We estimate that the melting point for the compressed cluster of 250 ST2 water molecules is 277 K. This estimate is based on the maximum of the apparent heat capacity derived from the curves of Fig. 1.

The core potential energy per particle ϕ_c is plotted in Fig. 2 for both the low pressure simulation[11] and the high pressure results of this study. The melting point is observed to shift downward by about 23 K, which compares quite favorably with the shift which occurs in water, viz., 22 K at 2 kbar.[13,14] Notice that as the fluid melts the pressure (see Table I) decreases, indicating a densification of the droplet.

Figure 3 shows the number of hydrogen bonds N_b and the number of molecules in the core N_c as a function of temperature. The hydrogen bond count decreases rapidly as the cluster is heated. The most rapid decrease occurs upon melting as expected. In addition, the core density increases upon melting as measured by N_c indicating a negative melting volume for ST2 water in bulk. This is a necessary but not sufficient property which any potential function purporting to model water molecules realistically should display.

Core and mantle hydrogen-bond distribution functions for the cluster at three different temperatures are shown in Fig. 4. The upper set of histograms give the distribution functions for the thermodynamic state at the specified temperature while the lower set of histograms give those for the states after quenching and will be discussed in the next section. The solid histograms show the hydrogen-bond distribution of molecules in the core while the shaded histograms show the mantle distributions. The tick marks along the ordinate indicate the number of hydrogen bonds with the shortest tick indicating zero bonds and the longest tick indicating six bonds. The histograms clearly show that the mantle is liquid-like even at low temperatures, i.e., 215 K, whereas the core region only becomes highly disordered at the melting point and above. These observations are consistent with the results of the low pressure study.[11]

IV. QUENCHING AND INHERENT STRUCTURES

The inherent structures or relative minima in the potential energy of a complex fluid such as water[15,16] are numerous and diverse. In fact, ice by itself is known to possess many different stable crystalline structures at various temperatures and densities.[16] The number of potential energy minima is very large and depends on the number of molecules N which comprise the system. There are $\approx 3^N N!$ minima for hexagonal ice alone, related by simple rotations and permutations of the water molecules. However, even discounting this permutation factor, general arguments[15] show that the total number of distinct minima rises exponentially fast with N.

It recently has been shown for a two-dimensional simple fluid[17] that the melting process may be explained by the change in the nature of the underlying inherent structures.

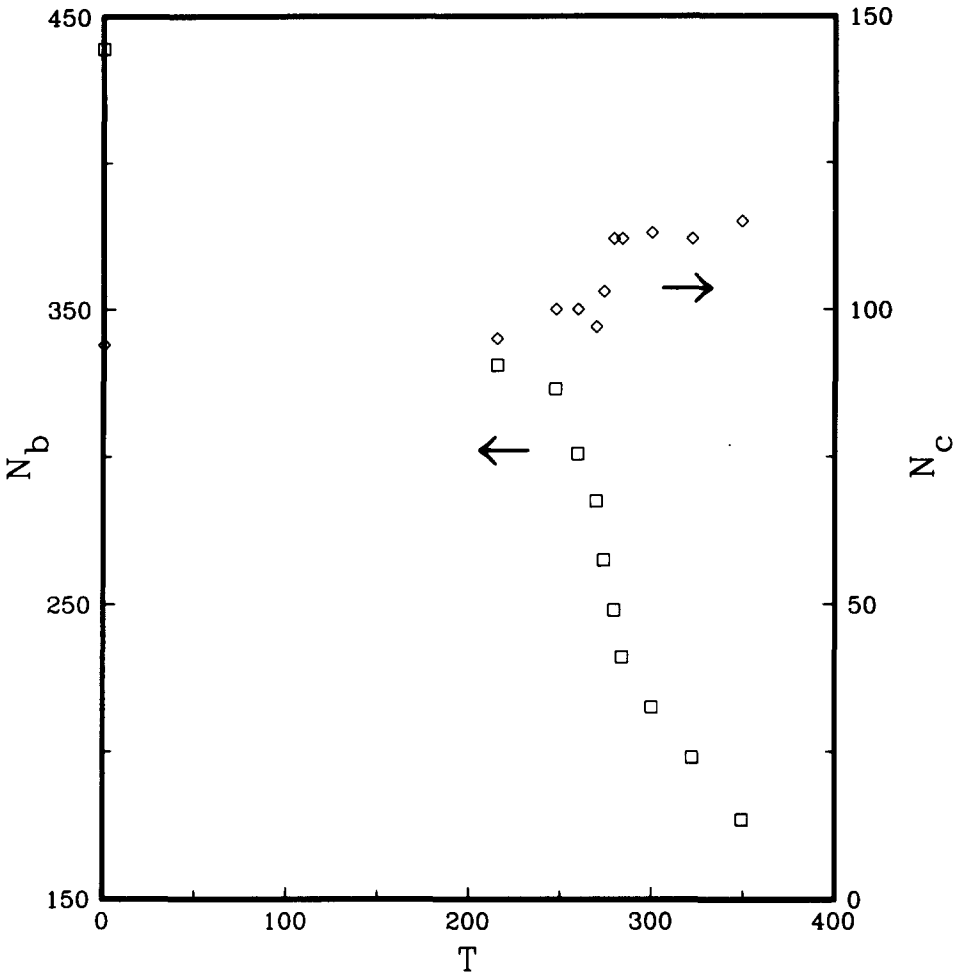

FIG. 3. N_b, the total number of hydrogen bonds of the 250-molecule cluster vs temperature. N_c is the number of molecules in the core of the cluster.

configuration for all water molecules in the droplet core (defined by a sphere of radius 9 Å as before), i.e., ϕ_{cq} is included in Table III and also plotted in Fig. 1.

From the graph of Fig. 1, it is possible to estimate the percentage of the latent heat of melting attributable to the shift in packing energy of the underlying inherent structures. We find using the core energy per particle plots that

$$\frac{\Delta\phi_{cq}}{\Delta\phi_c} \approx 0.87 \tag{4.3}$$

in good agreement with our previous ice melting studies[11] where we found 85%–90% of the latent heat was due to the change in the nature of the inherent packing structures. The remainder of the latent heat necessarily must be attributed to the difference in the vibration-libration anharmonicity between the liquid and the crystal.

Core and mantle hydrogen-bond distribution functions for the quenched clusters at three different temperatures are shown in the lower histograms of Fig. 4. From these it is obvious that the droplet core retains its crystalline structure up to the melting point whereas the mantle displays liquid-like character well below the melting point.

We have used linear least squares to fit the core potential energy of the five liquid state points. Before quenching, the result is (in kcal/mol)

$$\phi_c \approx 0.015\,87T - 14.7345, \tag{4.4}$$

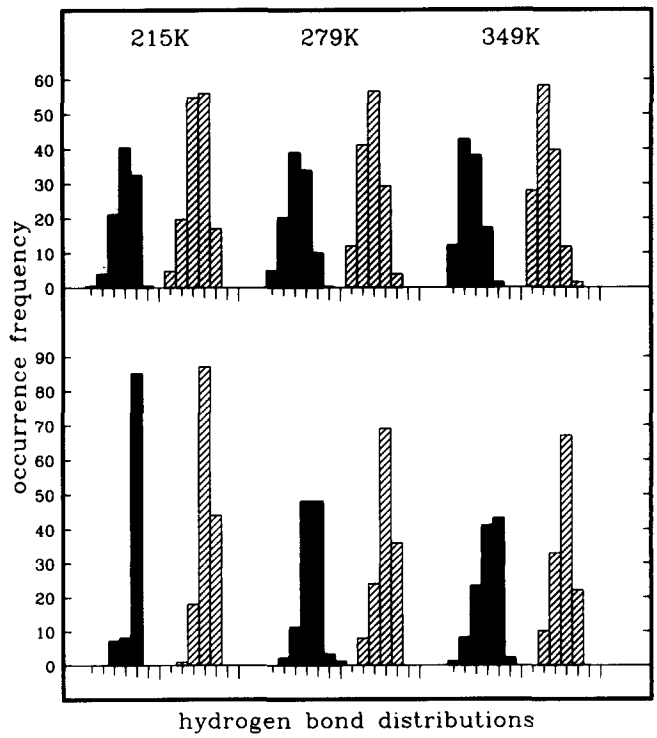

FIG. 4. Hydrogen-bond distributions of core (solid) and mantle (shaded) molecules at three temperatures: crystal, melting point, and liquid. The lower curves show the distributions of the quenched configuration. The number of hydrogen bonds (0,1,...6) are indicated respectively by the ticks of increasing length.

while after quenching

$$\phi_{cq} \approx 0.002\,592T - 13.3295. \quad (4.5)$$

The fits are meaningless at very low temperatures because at $T = 0$ K the potential energy determined from Eq. (4.4) is below that of the perfect crystal. Also the two curves cross at $T = 105.8$ K, which is impossible. However, the fits should provide a qualitative guide in the range from 250–350 K.

If the vibrational excitation removed by quenching were strictly harmonic, then the classical equipartition theorem requires:

$$(d/dT)(\phi_c - \phi_{cq}) = 3k_B = 0.005\,693 \text{ kcal/mol K}. \quad (4.6)$$

The actual difference determined from Eqs. (4.4) and (4.5) is

$$(d/dT)(\phi_c - \phi_{cq}) = 0.013\,277 \text{ kcal/mol K}, \quad (4.7)$$

which shows strong anharmonicity to be present. For the previous low pressure melting study[15] we found a value of 0.013 264 kcal/mol K for this last quantity. The restoring forces in the liquid on average are thus substantially weaker than harmonic.

V. SUMMARY AND CONCLUSIONS

The principle results of this study may be summarized as follows: (1) The external potential used to hold the droplet together may be used to compress the droplet. At a pressure of about 2 kbars we find a melting point depression of about 23 K, in excellent agreement with experiment. (2) As the fluid melts, the pressure decreases indicating that the liquid is more dense than the crystal. The droplet volume contracts on melting. (3) The droplet mantle is liquid-like well below the melting point of the crystal. (4) 87% of the latent heat of melting may be ascribed to the change in underlying inherent packing structures of the liquid. The latent heat is found to be 1.28 kcal/mol (experimentally equal to 1.13 kcal/mol[14] for ice at 2 kbars). (5) The remaining 13% of the latent heat arises from the difference in the anharmonicity of the fluid phase over the crystal.

This work represents the first simulation effort to melt an ice crystal under an applied pressure. The ST2 potential provides an adequate representation for the water molecules and we find good agreement with the experimental melting point depression as well as a density increase on melting.

[1] A. Rahman and F. H. Stillinger, J. Chem. Phys. **55**, 3336 (1971).
[2] F. H. Stillinger and A. Rahman, J. Chem. Phys. **60**, 1545 (1974).
[3] D. Matsuoka, E. Clementi, and M. Yoshimine, J. Chem. Phys. **64**, 1351 (1976).
[4] A. Rahman, F. H. Stillinger, and H. L. Lemberg, J. Chem. Phys. **63**, 5223 (1975).
[5] S. Swaminathan and D. L. Beveridge, J. Am. Chem. Soc. **99**, 8392 (1977).
[6] W. L. Jorgensen, Chem. Phys. Lett. **70**, 326 (1980).
[7] D. C. Rapaport and H. A. Scheraga, Chem. Phys. Lett. **78**, 491 (1981).
[8] A. Rahman and F. H. Stillinger, J. Chem. Phys. **57**, 4009 (1972).
[9] R. M. J. Cotterill, J. W. Martin, O. V. Nielsen, and D. B. Pedersen, in *Physics and Chemistry of Ice*, edited by E. Whalley, S. J. Jones, and L. W. Gold (Royal Society of Canada, Ottawa, 1973), pp. 23–27.
[10] T. A. Weber and F. H. Stillinger, J. Phys. Chem. **86**, 1314 (1982).
[11] T. A. Weber and F. H. Stillinger, J. Phys. Chem. (in press).
[12] D. J. Evans, Mol. Phys. **34**, 317 (1977).
[13] D. Eisenberg and W. Kauzmann, *The Structure and Properties of Water* (Oxford University, Oxford, 1969), p. 93.
[14] N. E. Dorsey, *Properties of Ordinary Water Substance* (Hafner, New York, 1968), p. 617.
[15] F. H. Stillinger and T. A. Weber, J. Phys. Chem. **82**, 2833 (1983).
[16] N. H. Fletcher, *The Chemical Physics of Ice* (Cambridge University, London, 1970).
[17] F. H. Stillinger and T. A. Weber, Phys. Rev. A **25**, 978 (1982).
[18] R. Fletcher, *Practical Methods of Optimization* (Wiley, New York, 1980).